Materials Today Electronics 3 (2023) 100026

Contents lists available at ScienceDirect

Materials Today Electronics

journal homepage: www.elsevier.com/locate/mtelec

Short Communication

Enhancing the bandwidth of antennas using polymer composites with high dielectric relaxation

Ilkan Calisir[a,1], Xiantao Yang[b,1], Elliot L. Bennett[a], Jianliang Xiao[a,*], Yi Huang[b,*]

[a] Department of Chemistry, University of Liverpool, Crown Street, Liverpool, L69 7ZD, United Kingdom
[b] Department of Electrical Engineering and Electronics, University of Liverpool, Brownlow Hill, Liverpool, L69 3GJ, United Kingdom

ARTICLE INFO

Keywords:
Antenna
Complex permittivity
Composite materials
Dielectric relaxation
Microwave devices
Polymer dielectric composites

ABSTRACT

We propose a concept using a frequency-dependent property (dielectric relaxation) of dielectric materials to enhance the bandwidth of the antenna widely used in wireless communications. The bandwidth enhancement can be achieved when a loading dielectric material with a relative permittivity that is inversely proportional to the frequency by the power of n. The bandwidth for a selected antenna example could be increased by 135% when the power $n = 2$. A solid material, composed of plasticized PVDF containing nano-sized silica particles, exhibiting dielectric relaxation of $n = 0.52$, is developed in order to prove the theoretical concept and used to test the performance of an example mobile phone antenna. The influence of hydrogen bonding on tuning the frequency-dependent power n in the developed composite material is verified. The bandwidth of the antenna was increased by 18% over the operating frequency band using a newly developed dielectrically relaxing material, $n = 0.52$ compared to the conventional non-relaxing material, $n = 0$.

1. Introduction

Wideband and compact antennas are needed in modern wireless communication systems for high performance and integration. Owing to the recent developments in the field of wireless communications, the demand for simple, reliable, economical, low profile, and light-weight broadband antennas has increased. Antennas allow the transmission and reception of radio waves as information signals and are essential electronic components widely used in mobile phones and base stations, which profoundly transform human lifestyles [1–3]. As multiple antennas for different bands make the system bulky and complicated, a single antenna covering a wider band becomes one of the most effective options. Therefore, researchers are focusing on developing better antenna designs with a wider bandwidth and smaller dimensions. Several techniques including the use of split-ring resonators [4], electromagnetic band-gap structures [5], slots in the ground plane [6], L-shaped feeding method [7], T-shaped slot patch antenna [8], loading the antenna with dielectric or magnetic material [9], and mushroom-shaped dielectric resonator antenna [10] *etc.* are employed for improving the bandwidth and/or gain of antennas. Nevertheless, these methods are not ideal for wireless communication systems due to their complexity.

In addition to good conductors, dielectric materials can also be used to make antennas. The selected dielectric materials are frequency-independent, temperature-stable and low-loss [1,11]. Therefore, the antenna development to enhance the bandwidth has relied on the creativity and tools used in the design process. On the material development side for wireless communications, the focus is mainly to obtain the high dielectric permittivity in order to reduce the antenna size [12], temperature stable microwave dielectric in order to be used in extreme/harsh environments [11], and low dielectric loss material (highest Q factor) [11] to maximize the radiation efficiency of the device. Metamaterials are the most recent materials used to improve the bandwidth [13] or reduce size [14]. However, they are normally of limited bandwidth and with increased complexity of the antenna; in many cases they actually increase the size of the antenna. Although a lot of progress has been made, the demand for wideband microwave devices and antennas is still not well met.

A common method to downsize an antenna is to enhance the dielectric permittivity of material *via* doping or a composite approach, namely combining various materials such as polymers, ceramics and metals. Currently, dispersing a high dielectric constant ceramic powder, *e.g.*, lead-containing compounds ($PbTiO_3$, $Pb(Zr,Ti)O_3$, or $Pb(Mg_{1/3}Nb_{2/3})O_3$-$PbTiO_3$) or lead-free compounds ($CaCu_3Ti_4O_{12}$, $BaTiO_3$) into the polymers to form 0-3 type composites is a proven method to enhance the dielectric permittivity [15]. Incorporation of metal particles such as Ni [16] and Ag [12] in various sizes/shapes into the polymer matrix is also found to greatly increase the dielectric permit-

* Corresponding authors.
E-mail addresses: jxiao@liverpool.ac.uk (J. Xiao), huangyi@liverpool.ac.uk (Y. Huang).
[1] I.C. and X.Y. contributed equally to this work.

https://doi.org/10.1016/j.mtelec.2023.100026
Received 25 November 2022; Received in revised form 27 January 2023; Accepted 13 February 2023
Available online 15 February 2023

tivity and resulting composites are suggested to be promising candidates in antenna miniaturization.

Dispersive materials are defined as the material whose permittivity changes as a function of frequency, thus the velocity of a radio wave in the material is also a function of frequency. It was theoretically predicted that the bandwidth of a small antenna could be increased by using dispersive materials [17,18]. Herein we propose a new concept that utilizes a material whose relative permittivity is inversely proportional to the frequency by the power of n so as to improve the antenna bandwidth. According to this concept, the relative permittivity $\varepsilon_r(f)$ can then be expressed as,

$$\varepsilon_r(f) = \frac{k}{f^n} \tag{1}$$

where k is a material-specific coefficient, and f is the frequency. This concept requires a dielectric material possessing high dielectric relaxation behaviour. To our knowledge, this is the first time materials with dielectric relaxation have been taken advantage of for wireless microwave devices, where such nonlinearity in permittivity/capacitance as a function of frequency (within the operating frequency range) is often not desired. Antenna miniaturization is conceivable using the proposed concept, as the higher permittivity of a material with high power n, the smaller antenna size and wider bandwidth can be achieved.

To materialize this concept, a material with dielectric relaxation in the microwave region is required. Therefore, we focused on materials with high polarity. Typically, all polar materials are expected to show dielectric relaxation (also referred to as microwave dielectric dispersion) in the microwave region since they are comprised of dipoles and the orientation of dipoles is sensitive to the alternating electric field. Electroactive polymers such as poly(vinylidene fluoride) (PVDF) are therefore good candidates owing to the high electronegativity of fluorine that makes the C–F bond highly polar. They are utilized in many electronic applications since they exhibit good piezoelectric/pyroelectric responses and low acoustic impedance, which matches water and human skin, and additionally, their properties can be tailored to meet various requirements [15,19].

In this communication, we report a novel kind of ferroelectric polymer-based composite with high dielectric relaxation and good flexibility, prepared using a simple blending procedure. Our composites are based on the combination of PVDF ferroelectric polymer plasticized with propylene carbonate (PC), and filler particles. Cheap and readily available silica gel was selected as an inorganic filler due to the presence of hydroxyl groups on the surface which can interact with the polymer matrix through hydrogen bonding and can strengthen the dielectric relaxation of the system. The enhancement observed in the dielectric relaxation of the composites is elucidated by the increased concentration of hydrogen bonding in the system [20–22]. The newly developed material is then fabricated into a real device prototype in order to test the improvement of the antenna performance within the investigated frequency band. This new concept and the relevant theoretical background are presented in the following section.

2. Concept and theoretical background

Generally, the relative permittivity of traditional materials used in wireless devices is frequency-independent in the microwave region. Thus, the electrical length is frequency-dependent for a determined physical structure which leads to the intrinsic narrow-band characteristic. Therefore, a new material that is frequency-dependent can be explored to obtain bandwidth enhancement, which has been particularly found to be an effective tool after our investigation for improving the operating bandwidth of wireless communication systems.

To begin with, a simple example of a slot antenna is illustrated in Fig. 1a. The antenna is constructed with a slot of length l and width w in a big conducting ground plane. Usually, the slot perimeter is around one wavelength of the operating frequency. To downsize the slot, the dielectric material can be loaded on one side of the slot. Normally a larger size dielectric material is needed for resonating at a lower frequency, while a smaller size is required for a higher frequency when using traditional frequency-independent materials, as illustrated in Fig. 1b and c. Thus, different antennas must be used to cover different frequency bands which makes the system complicated and bulky. On the other hand, it is feasible to use a simple antenna with a determined size to cover a large band utilizing the new material with varying power n, as shown in Fig. 1d.

The relationship between the wavelength and power n is given in Fig. 1e within the frequency range of 0.6 to 1.0 GHz. It can be seen that the slope of the wavelength curve becomes smaller when the power n increases and is almost constant when $n = 2$, which indicates that the bandwidth of the slot antenna can be improved with increasing n ($n \leq 2$). Thus, this inverse relationship between the wavelength slope and the power n can be now explored to obtain greater antenna performance with a larger bandwidth. It should be noted that when the power n is higher than 2, the slope becomes larger in the opposite direction, and this case is not considered in this paper since the bandwidth enhancement is reversed. In our recent simulation work [23], a mobile phone antenna was designed using the new material with $n = 2$. Using the new relation expressed in Eq. 1, the new simulated results of the bandwidth enhancement based on the mobile phone antenna loaded with materials exhibiting different power n are shown in Fig. 1f. It can be seen that the greater the power n, the larger the bandwidth increase, which demonstrates the improvements from this new type of material and further verifies the proposed concept which is applicable to wideband wireless communication systems.

In this work, we only need to consider the dipolar type of polarisation in a dielectric material since it induces the dielectric relaxation in the microwave region, although there are other polarisation mechanisms involved in relaxation as well as resonance in a different region of the dielectric spectrum (Fig. S1 in the ESI). In detail, at frequencies below dielectric relaxation, the rate of change of the alternating electric field is slow enough to allow the dipole reorientations to keep up. As the frequency increases, a time-lag between the dipole alignment and the oscillating electric field begins to develop; as a result, the real part of the permittivity decreases rapidly. At frequencies well above the relaxation frequency, both real and imaginary parts of the permittivity decrease, since orientation polarizability ceases to be a predominant mechanism due to the dipole rotation effectively *not in sync* with higher frequency in the electric field [24].

Broadband dielectric spectroscopy is a versatile technique that can measure dielectric properties including dielectric relaxation. The complex permittivity of dielectrics is a frequency-dependent property and it can be mathematically expressed by Eq. 2, known as the Debye model, using ε_s (static permittivity), ε_∞ (infinite permittivity), τ (relaxation time) and ω (angular frequency). The parameters ε_s, ε_∞ and τ, in the Debye equation are material-specific constants and intrinsic properties of all dielectrics [24]. This equation can be further divided into real (Eq. 3) and imaginary (Eq. 4) terms, and mathematically allows us to model the dielectric relaxation of a material.

$$\varepsilon_r = \varepsilon_\infty + \frac{\varepsilon_s - \varepsilon_\infty}{1 + j\omega\tau} \tag{2}$$

$$\varepsilon^{/} = \varepsilon_\infty + \frac{\varepsilon_s - \varepsilon_\infty}{1 + \omega^2\tau^2} \tag{3}$$

$$\varepsilon^{//} = \varepsilon_\infty + \frac{(\varepsilon_s - \varepsilon_\infty)\omega\tau}{1 + \omega^2\tau^2} \tag{4}$$

The angular frequency is $\omega = 2\pi f$ and the dielectric relaxation strength is defined as $\Delta\varepsilon = \varepsilon_s - \varepsilon_\infty$ and accounts for the orientational polarizability of a dielectric. When these two terms are placed into the Debye equations Eqs. 2 and (3) we can clearly see the power relation of frequency with respect to both real and imaginary parts of permittivity as given in the rearranged Eq. 5. This relation can, to a certain extent, confirm the feasibility of the proposed concept based on the equation of

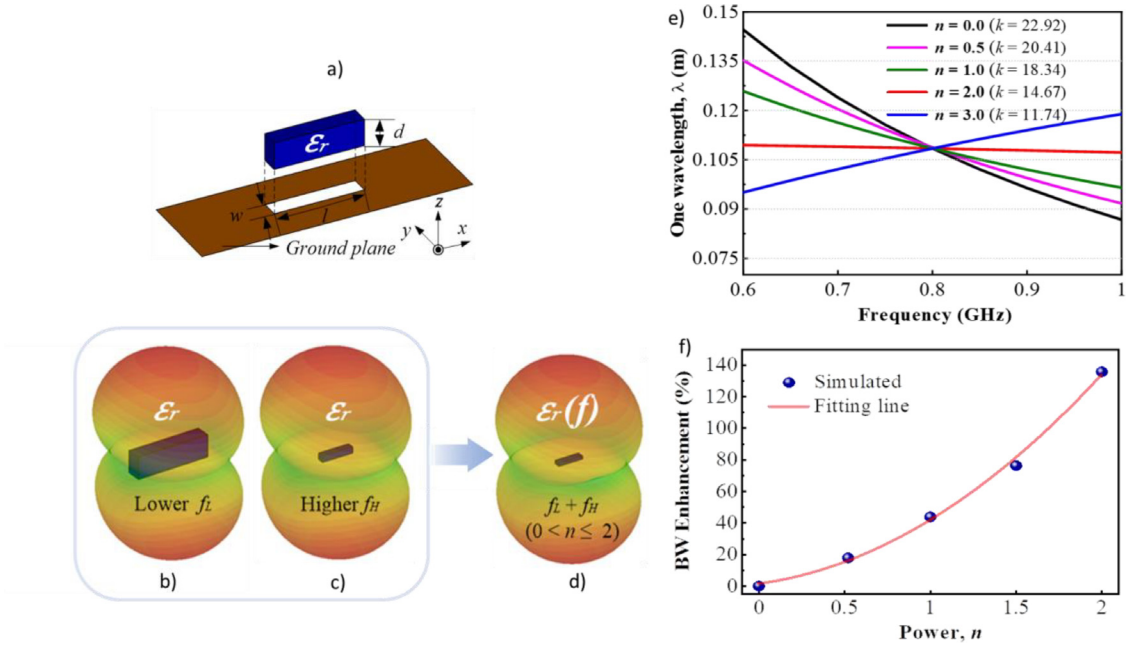

Fig. 1. Concept illustration using an example slot antenna for wideband wireless communication. a) Slot antenna with a slot in a big ground plane where dielectric material can be loaded on one side of the slot; b) a larger dielectric block is used for operating at a lower frequency band; c) a smaller dielectric block is used for operating at a higher frequency band; d) wider bandwidth is achieved by loading the new material. The colored shape around the slot and dielectric block denotes the radiation pattern of the antenna. The red area is shown as the strongest radiation direction originated from the antenna. Simulated results based on the power relation given in Eq. 1: e) The relationship between the wavelength and operating frequency for the materials with various power n ($0 \leq n \leq 3$); f) Bandwidth (BW) enhancement of a mobile phone antenna as a function of the power of frequency, n.

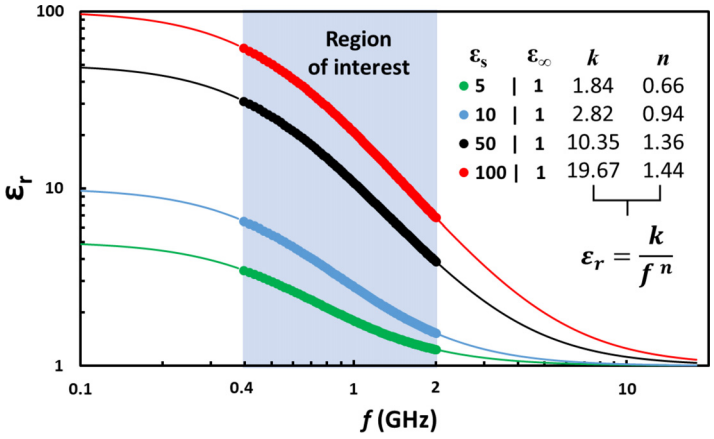

Fig. 2. Simulated dielectric profiles using Debye function as a function of various ε_s and fixed ε_∞. Highlighted region from 0.4 to 2 GHz is fitted using the proposed power equation (Eq. 1) and fitting parameters, n and k values are given in the inset.

$\varepsilon_r(f) = \frac{k}{f^n}$.

$$\varepsilon' - \varepsilon_\infty = \frac{\Delta\varepsilon}{1 + 4\pi^2 f^2 \tau^2} \quad (5)$$

To gain further insight into the dielectric relaxation of a polar material, a simple simulation using Debye equation (Eq. 5) with the various values of ε_s and a fixed ε_∞ was performed and the results are shown in Fig. 2. The simulation yielded various relaxation curves and when the curves within the targeted frequency band (0.4 GHz to 2.0 GHz) was fitted using the Eq. 1, it can be seen that the power n increases from 0.66 to 1.44 as the static permittivity (ε_s) of a material increased in respect to (ε_∞) as illustrated within the inset of Fig. 2. This provides an important guide for the dielectric material selection/development in order to tune the power n for a desired frequency range to be used in the proposed concept.

Although the Debye relaxation model is proposed to describe the behavior of polar dielectrics at various frequencies, in reality, very few materials completely agree with Debye equations [24]. The discrepancy is attributed to what is generally referred to as the *distribution of relaxation times*. The Debye theory describes materials with a single relaxation time. The accuracy of the model is reduced when there is more than one relaxation time present, such as in mixtures or composite materials. There are several modified dielectric models which better describe more complex materials and composites including Cole-Cole, Davidson-Cole and Havriliak-Negami [24,25].

A material was then designed and prepared to satisfy the relaxation concept outlined above.

3. Results and discussion

Herein, PVDF polymer was used as a matrix material that exhibits dielectric relaxation in the microwave region due to its ferroelectric (polar) nature. However, the dielectric properties of pure PVDF, $\varepsilon_r = 3.5$ at 0.2 GHz and relaxation strength $\Delta\varepsilon = 0.53$ (0.2 to 10 GHz) yielding a power $n = 0.06$, are not sufficient for the proposed concept. Therefore, its dielectric properties must be modified using either different

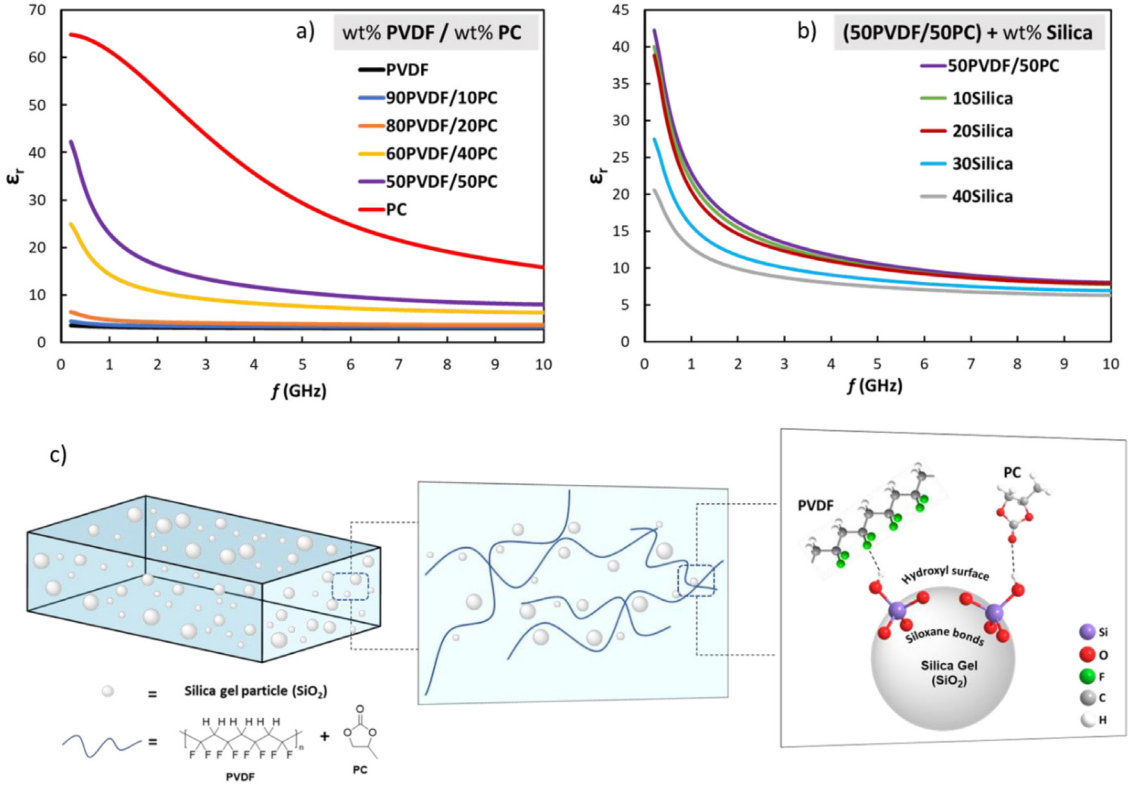

Fig. 3. Dielectric spectra of a) *x*PVDF–(*100-x)* PC (*x* in wt%) composite, b) (50PVDF/50PC) + *x* wt% silica, and c) Sketch of silica-filled PVDF/PC composite, illustrating hydrogen bonding between the hydroxyl donor groups on the surface of silica particle and acceptor groups of PVDF/PC molecules, shown as dashed lines.

processing techniques [19] or by adding other materials including organic/inorganic additives [16,19].

A common plasticizer propylene carbonate (PC), which has a high relative permittivity $\varepsilon_r = 64.5$ at 0.2 GHz and high dielectric relaxation strength $\Delta\varepsilon = 50$ over the frequency range 0.2 to 10 GHz, was selected. The main role of the plasticizer PC in PVDF is to increase the dielectric relaxation, however, it can also substantially improve the physical properties since it can soften the polymer backbone promoting higher segmental motion of polymer chains. This softening behaviour is found to be useful when ionic conductivity is highly desired, due to assisting the transportation of ions through the polymer. Thus, a PC plasticized polymer matrix is often preferred as a gel polymer electrolyte in Li-ion batteries [26].

The permittivity of a modified PVDF matrix with various wt% of PC as a function of frequency is shown in Fig. 3a. It can be seen that dielectric relaxation was improved by incorporating PC up to 50 wt% into PVDF. At 50PVDF/50PC composition, the physical properties changed dramatically and became softer and slightly tacky indicating excessive addition of PC. This physical state limited the processability of the material and caused instability during dielectric measurements. This issue is overcome by incorporating nano-sized silica particles as an inorganic filler. As received micron-sized silica gel particles (40-63 μm) were milled using high-energy ball milling, nano-sized silica particles were achieved as can be seen in Fig. S2(ESI). The milled silica was then added to 50PVDF/50PC polymeric matrix in up to 40 wt%. The variations in the permittivity are shown in Fig. 3b. The permittivity of nano-sized silica particles is found to be 2.3 - 2.9 in the range of 0.2 - 10 GHz as given in Fig. S2a (ESI) which show an amorphous structure confirmed by XRD (Fig. S2b in the ESI). Therefore, a reduction in permittivity is expected when increasing the silica concentration as seen in Fig. 3b. However, the dielectric relaxation as quantified by the power *n* in 10Silica is almost maintained, yielding a similar value to the polymeric matrix of 50PVDF/50PC, with the highest relaxation observed in the 20Silica composite. This enhancement is attributed to the increased intermolecular hydrogen-bonding between the hydroxyl donor groups on the surface of silica (–OH) with the acceptor groups of PVDF (C–F) and PC (C=O) as illustrated in Fig. 3c. The degree of hydrogen-bonding between them increases with an increasing amount of silica up to 20 wt%. More silica addition resulted in an apparent decrease in the permittivity as well as relaxation strength which might be due to exceeding the threshold of effective interfacial hydrogen bonding formation, with the excess low permittivity silica now reducing the overall permittivity. The C–F bonds in PVDF are able to act as hydrogen bond acceptors, forming hydrogen bonds with the silanol groups on the surface of silica (SiO_2) [27–29]. Therefore, silica can act as a dielectric relaxation enhancer within PVDF and PC, up to a certain wt%. It is also reported that when silica is uniformly coated on PVDF particles in the form of core-shell, electroactive phases in PVDF, namely, β- and γ-phases, and its polarity are suppressed due to the formation of vinyl groups on the silica shell [30]. Nonetheless, in our case, silica particles are not coated on the PVDF particles, instead they are uniformly dispersed in the polymeric matrix; therefore the suppression of electroactive phases and polarity of PVDF is not expected. PVDF and PC can simultaneously interact with −OH groups on the surface of silica through hydrogen bonding. In this context regarding hydrogen-bonding and induced polar phases in PVDF-based composites, both Fourier transform infrared spectroscopy (FT-IR) and X-ray diffraction (XRD) analyses were carried out and the results are discussed in the following part.

Neat PVDF may contain various crystalline polar and nonpolar phases depending on the processing methods [31,32]. XRD results (Fig. S3 in the ESI) show that the crystalline phases of neat PVDF powder assigned as α, β and γ exhibit weak intensity, while upon addition of PC up to 50 wt% (50PVDF/50PC), the peak intensities increase and characteristic peaks of polar and nonpolar phases are detected. This indicates that PVDF/PC composites may contain both nonpolar and polar phases. Nonetheless, adding 20 wt% milled silica to 50PVDF/50PC resulted in

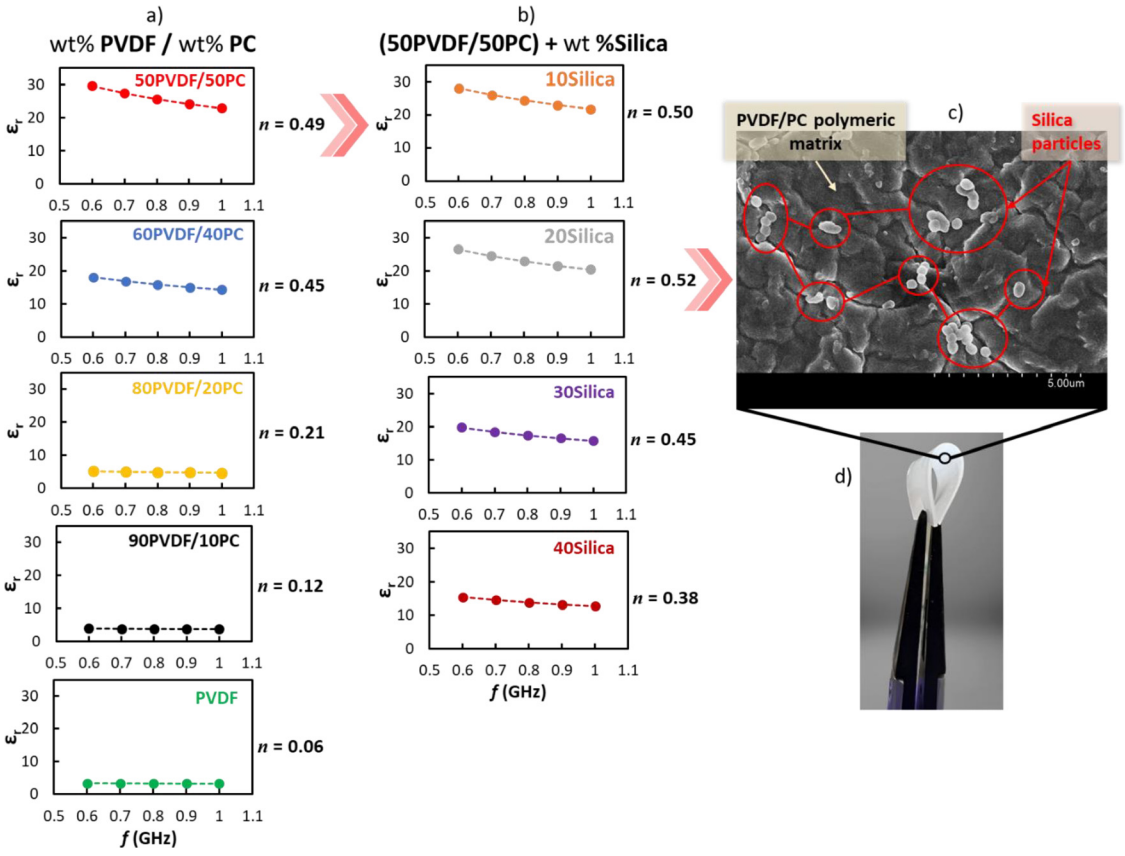

Fig. 4. a) Relative permittivity profiles of PVDF/PC (wt%) and b) (50PVDF/50PC) + *x* wt% silica composites from 0.6 to 1.0 GHz. c) SEM image of (50PVDF/50PC) + 20 wt% silica composite and d) photographic image of the flexible composite.

the disappearance of nonpolar α phase and confirmed the presence of polar β and γ phases, which is also validated by FT-IR absorbance data (Fig. S4b in the ESI). The peaks of β and γ phases in both XRD and FT-IR data are overlapped due to similar polymer chain conformation [31] and therefore we treat them as one polar phase ($\beta + \gamma$). On the other hand, the nonpolar α phase is clearly identified in both analyses. Upon 40 wt% milled silica addition (40Silica), the peak intensities in the XRD profile were significantly dropped. The present phases could no longer be distinguished since the increased amorphous silica addition broadened the peaks. Having a higher concentration of polar phases in the PVDF composite is found to be important for dielectric relaxation response, since the higher the polarity, the larger relaxation response can be obtained [32], as it is also shown in our result.

The FT-IR spectra of PC and milled silica added PVDF composites (Fig. S4 in the ESI) in the regions of 2800 to 3100 and 3100 to 3700 cm^{-1} were analyzed in order to monitor CH_2 and –OH stretches, respectively, which could be used as an indication of hydrogen bonding between each component of the composite [27]. A slight frequency shift in CH_2 stretching was observed when PC and milled silica are added to PVDF, although the PC peak is overlapped and masks the accurate position of the peaks. In –OH stretching region, a broad absorption band is attributed to the hydrogen-bonding hydroxy groups. With increasing the milled silica content up to 40 wt%, the peak near 3300 cm^{-1} slightly broadened and became more pronounced when the milled silica addition is at 40 wt%.

These results indicate that hydrogen bonds are most likely to be formed between the surface of milled silica particles and PVDF-PC polymer matrix, and the polarity of the PVDF-based composites is increased by the addition of solid silica particles. The hydrogen bonding at the interfaces between silica surface and PVDF molecules together with dipolar interactions between PVDF and PC tend to generate locally oriented dipoles which promote polarity, and dielectric relaxation accordingly. This was confirmed electrically by dielectric spectrum given in Fig. 3a-b and structurally by XRD and FT-IR data (Fig. S3 and S4 in the ESI).

To gain further insight into the dielectric relaxation behaviour of the composites, their power *n* was analysed from 0.2 to 10 GHz. After inspection, it is found that highest powers of *n* can be obtained in the region of 0.6 to 1.0 GHz. The dependence of the power *n* and compositions are shown in Fig. 4a. The power *n* increased from 0.06 to 0.49 by adding PC up to 50 wt%, and then it further increased to 0.52 when 20 wt% silica was added to the 50PVDF/50PC matrix, as shown in Fig. 4b. Such enhancement was explained by the contribution of hydrogen-bonding discussed previously. Fig. 4c shows a typical microstructure of the silica-added PVDF/PC composites, in which the polymer is self-connected into a continuous network and the silica particles are randomly distributed within the polymeric matrix. The flexibility of the obtained composite is also illustrated in Fig. 4d.

As pointed out in Fig. 1f, it is important to have a material with a high power of *n* to enhance the bandwidth up to 135%. The obtained results show that tuning the power of *n* through PC and silica addition to PVDF is viable and a maximum value of *n* can be obtained in this material system (0.52), which is expected to show an 18% bandwidth increase based on the simulated results shown in Fig. 1f.

A mobile phone antenna prototype is illustrated in 3D with the dimensions shown in Fig. 5a. Following the required material and substrate dimensions, a prototype antenna was then fabricated as illustrated in Fig. 5b. A thin and flexible composite (2 mm x 2 mm x 80 mm), as demonstrated in Fig. 5c, was placed in the slot and the reflection coefficient is measured. Fig. 5d shows the simulated and measured reflection coefficients of the mobile phone antenna. The reflection coefficients are a good measure of how much power is reflected back from the antenna system, and a smaller reflection coefficient is usually required for the

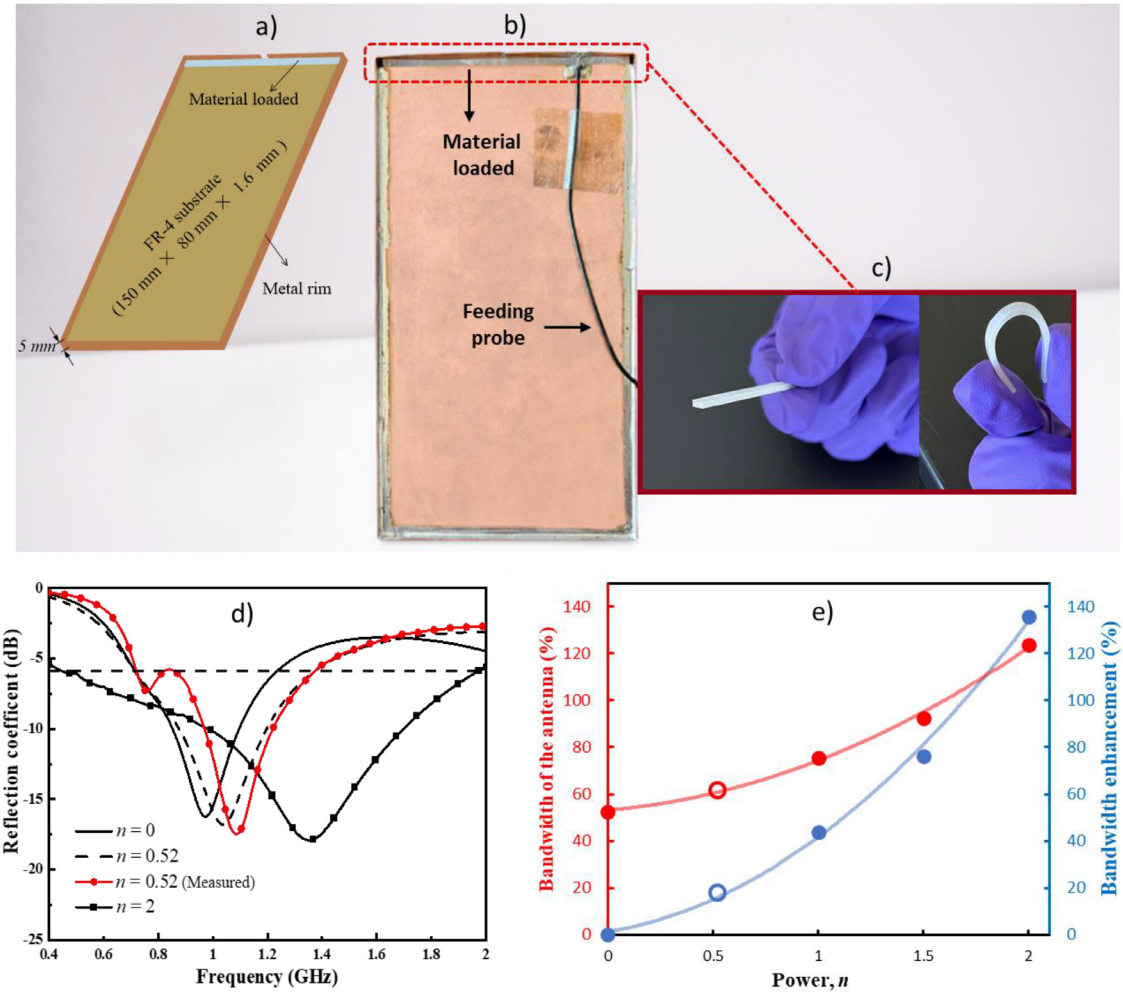

Fig. 5. a) 3D Illustration of mobile phone antenna configuration; b) photograph of fabricated mobile phone prototype with the material loaded; c) photographs of composite used in the device shown in b; d) The measured and simulated reflection coefficients result of the mobile phone antenna; e) Results of bandwidth of the antenna (%) and enhancement (%) as a function of frequency power *n* obtained from (d). Empty and filled data points represent the actual measured and simulated results, respectively.

communication system [33]. For the mobile phone antenna, -6 dB is normally the criterion for defining the effective operating band [33]. As can be seen from Fig. 5d, the measured bandwidth covers from 0.721 GHz to 1.366 GHz, which has a very good agreement with the simulated results, covering from 0.720 GHz to 1.365 GHz. This verifies the accuracy of the simulation and design, as well as the feasibility of the proposed concept and theory. Compared with the antennas loaded with traditional materials ($n = 0$), the bandwidth can be further improved using the materials with a larger power *n*. For example, a larger bandwidth is expected using the material with power, $n = 2$, which covers nearly from 0.4 GHz to 2 GHz, meaning the bandwidth can be improved by nearly 135% Fig. 5e.

It should be pointed out, that even though only one smartphone antenna was used as an example to demonstrate the usefulness of the proposed new material for antenna bandwidth improvement, the approach is general and suitable for most antennas. How much improvement can be achieved is directly related to the power of *n*. The antenna efficiency is another important aspect that must be taken account during antenna development. The efficiency is directly linked to the energy loss of the loading material which is associated with the imaginary part of permittivity (ε") where the stored energy corresponds to the real part of the permittivity (ε'), which is gradually or rapidly lost and dissipated as heat as the frequency increases in the microwave region. Particularly, the energy loss is maximum in the vicinity of the relaxation frequency, depending on the dominant polarisation mechanism of the used material. Therefore, dielectric loss, tan $\delta = \varepsilon"/\varepsilon'$, is a good indicator for the antenna efficiency. Dielectric losses of the developed composites in this work are given in Table S1 and S2 in the ESI. The dielectric loss of pure PVDF in the investigated frequency range from 0.4 – 2.0 GHz is found to be 0.08 – 0.09, whereas adding PC to PVDF as a plasticizer increases its dielectric loss to 0.75 in the trade-off to achieve higher power *n*. Increasing the wt% of nano-sized silica particles in the 50PVDF/50PC composite reduced its dielectric loss to between 0.36 – 0.52. Nonetheless, the composite with the highest power ($n = 0.52$) exhibited a dielectric loss of 0.47 – 0.73, between 0.4 – 2.0 GHz. This result is also in agreement with existing dielectric relaxation models, which suggest that higher dielectric relaxation (power *n*) results in higher dielectric loss. The antenna efficiency is therefore expected to be low due to the relatively high dielectric loss (tan $\delta > 0.1$) obtained in the developed composites which is -14.7 dB at 0.8 GHz as given in the Fig. S5. This is the most challenging issue and possible limitation of this concept for the applicability, not only for this type of antenna but also general classes of antennas, and efforts to reduce the dielectric loss while increasing the power *n* is under development.

Material development for this proposed concept is in its infancy. Especially, in solid materials, it may be challenging to achieve a high power of frequency *n*, since the dipolar/orientational polarisation could be limited by intrinsic and extrinsic factors, including restricted or

orientational-dependent polarisation by molecular and crystal structures, structural/charged defects, interfacial interactions in composites and processing methods. Nevertheless, it is reported that the relaxation frequency and the magnitude of permittivity can be tuned *via* doping methods in certain ferro (piezoelectric) ceramics such as $BaTiO_3$ [34], $NaNbO_3$ [35], and $Pb(Zr,Ti)O_3$ [36]. Dispersing carbonaceous materials including activated carbon, carbon nanotubes, graphene into the polymer and/or ceramic matrix is also reported to improve the dielectric relaxation behaviour of a composite [37,38]. However, this introduces an additional conductivity term to the Debye model, resulting in an increase in dielectric relaxation, but also in the conductivity which is not desired in the required antenna specifications. Due to the strong intermolecular hydrogen bonding in many molecular liquids, high dielectric relaxation is expected such as in alcohols [20] and amides [39]; therefore the dielectric spectrum of polar liquids is closer to be fit to the Debye model, yielding sharper dielectric relaxation (higher power n as shown in Fig. 2), as compared to solid polar type of polymers and ceramics, or polymer-ceramic-metal composites. Thus, compositional trials based on the current dielectric material literature (in solid or liquid form) supported by the dielectric relaxation models are crucial to find a material exhibiting higher power n.

Data-driven techniques have been recently found to be popular and powerful alternatives to effectively bypass these exhausting experimental trials, by building surrogate models for property prediction (*e.g.* dielectric permittivity and loss) and material design, which can potentially accelerate the discovery and application of new materials [40,41]. Recently, machine learning framework was explored in the area of frequency-dependent dielectric properties in polymers [42], microwave dielectric ceramics [43], and polymer-based composites [44]. Since our concept can only work with a material with high dielectric relaxation at the microwave region (*i.e* having high power n), a machine learning framework could be also utilized to design or discover a novel dielectric to fit our purpose, by searching and correlating essential parameters including hydrogen bonding capability, molecular structure, static permittivity, infinite permittivity, and relaxation time that are found to play a key role in dielectric relaxation.

4. Conclusions

A new concept to broaden the bandwidth of an antenna using a material having a high degree of dielectric relaxation is proposed. This concept is constructed on a frequency-dependent material whose relative permittivity is inversely proportional to the frequency power of n; $\varepsilon_r(f) = \frac{k}{f^n}$. Simulated results show this concept can potentially widen the operating bandwidth up to 135% when the power $n = 2$, compared to current traditional frequency-independent materials for which $n = 0$. Based on this proposal, a new material guided by dielectric relaxation theory is fabricated. The new material is a nano-sized silica-filled PVDF plasticized with PC and its power n reached up to 0.52, yielding an 18% improvement in the investigated bandwidth, which was tested and simulated in a prototype smartphone antenna. Thus, this proposed concept combined with theory and material development shows great potential for antenna applications in telecommunications.

5. Experimental section

All starting materials were purchased from Merck and Alfa Aesar and used without further purification unless otherwise stated. All manipulations and formulations were performed under an inert nitrogen atmosphere. The host polymer, as-received poly(vinylidenefluoride) (PVDF) and plasticizer propylene carbonate (PC, MW=102.09 g mol^{-1}) in various wt% ratios, were dissolved in the organic solvent dimethyl carbonate (DMC), 30 mL per 10 g of polymer composite, at 80°C until a clear viscous solution was obtained. The solvent DMC was removed *in vacuo* and the PVDF/PC was obtained as a white translucent polymer. Silica gel (40-63 μm) was milled in a high-energy planetary ball mill (Fritsch, Pulverisette 6) with a speed of 400 rpm for 2 hours using 1 mm diameter zirconia balls. Nano-sized silica particles were obtained after the milling procedure as shown in Fig. S2d. Milled silica was then added to the composite mixture before dissolution with DMC, and heated at 80°C under ultrasonication for 1 hour. After the removal of the solvent *in vacuo*, the obtained dried composite material was cut into small pieces and ground using a mill (IKA A11) producing a fine powdered composite. The fine powder was then hot-pressed in a stainless-steel die at 180°C for 20 minutes. Based on the required sample dimensions (2 mm x 2 mm x 80 mm) for the device prototype, the samples were then sliced into bar-shapes.

Hitachi S-4800 cold-field emission scanning electron microscopy (FE-SEM) was used for analysis of the samples' morphology. Prior to SEM, the sample surfaces (fracture cross sections, particle surfaces, natural surfaces) were coated with gold by Quorum S150T ES sputter coater. X-ray diffraction (XRD) results were obtained using a Bruker D8 Discover X-ray diffractometer with Cu-Kα radiation. The samples were scanned in the 2θ range of 5° to 80° with a step interval of 0.01314°. Fourier-transform infrared (FT-IR) spectroscopy tests covering the range of 550–4000 cm^{-1} were carried out using Perkin Elmer Spectrum 100 fitted with a universal attenuated total reflection (ATR) sampling accessory.

For dielectric measurements, the dielectric assessment kit for thin layers (DAK-TL2) from SPEAG (Schmid & Partner Engineering AG, Switzerland), which is based on the open coaxial probe method, was used to perform dielectric spectroscopy. The DAK3.5-TL2 probe (0.2 GHz - 20 GHz) was used in combination with a ZVL (Rohde & Schwarz, Munich, Germany) to perform measurements over the aforementioned frequency range. The measurement resolutions are set to 100 MHz covering the range from 0.2 GHz to 10 GHz. The DAK-TL2 system was calibrated using the standard 3-point calibration prior to each measurement session: open, short (copper strip), and de-ionized water as the load. A force of 500 N was applied during the short calibration to ensure a good contact between the probe and the copper strip.

The reflection coefficient of the mobile phone antenna was evaluated using a vector network analyzer (MS46322B Anritsu) covering the operating frequency band of antenna (0.4 to 2.0 GHz). CST Microwave Studio is employed here for the simulation and optimization which is based on the finite integration technique [45].

Data Availability

Data will be made available on request.

Acknowledgement

This work was supported by Huawei Technologies Co. Ltd., and the authors acknowledge their financial support.

Supplementary materials

Supplementary material associated with this article can be found, in the online version, at doi:10.1016/j.mtelec.2023.100026.

References

[1] M.T. Sebastian, Dielectric Materials for Wireless Communication, 2008.
[2] J. Martinez-Vega, Dielectric Materials for Electrical Engineering, Wiley-ISTE, 2013.
[3] Z. Xie, R. Avila, Y. Huang, J.A Rogers, Flexible and stretchable antennas for biointegrated electronics, Adv. Mater. 32 (2020) 1902767.
[4] Z. Jiang, et al., Wideband loop antenna with split-ring resonators for wireless medical telemetry, IEEE Antennas Wirel. Propag. Lett. 18 (2019) 1415–1419.
[5] D.N. Elsheakh, H.A. Elsadek, E.A. Abdallah, H. Elhenawy, M.F Iskander, Enhancement of microstrip monopole antenna bandwidth by using EBG structures, IEEE Antennas Wirel. Propag. Lett. 8 (2009) 959–962.
[6] R. Zaker, C. Ghobadi, J Nourinia, Bandwidth enhancement of novel compact single and dual band-notched printed monopole antenna with a pair of L-shaped slots, IEEE Trans. Antennas Propag. 57 (2009) 2187–2189.
[7] C.L. Mak, K.M. Luk, K.F. Lee, Y.L Chow, Experimental study of a microstrip patch antenna with an L-shaped probe, IEEE Trans. Antennas Propag. 48 (2000) 777–783.

[8] R.K. Verma, D.K Srivastava, Bandwidth enhancement of a slot loaded T-shape patch antenna, J. Comput. Electron. 18 (2019) 205–210.
[9] A.O. Karilainen, P.M.T. Ikonen, C.R. Simovski, S.A Tretyakov, Choosing dielectric or magnetic material to optimize the bandwidth of miniaturized resonant antennas, IEEE Trans. Antennas Propag. 59 (2011) 3991–3998.
[10] R. Cicchetti, A. Faraone, E. Miozzi, R. Ravanelli, O Testa, A high-gain mushroom-shaped dielectric resonator antenna for wideband wireless applications, IEEE Trans. Antennas Propag. 64 (2016) 2848–2861.
[11] I.M. Reaney, D Iddles, Microwave dielectric ceramics for resonators and filters in mobile phone networks, J. Am. Ceram. Soc. 89 (2006) 2063–2072.
[12] T. Inui, H. Koga, M. Nogi, N. Komoda, K Suganuma, A miniaturized flexible antenna printed on a high dielectric constant nanopaper composite, Adv. Mater. 27 (2015) 1112–1116.
[13] R. Yang, Y. Xie, D. Li, J. Zhang, J Jiang, Bandwidth enhancement of microstrip antennas with metamaterial bilayered substrates, J. Electromagn. Waves Appl. 21 (2007) 2321–2330.
[14] W. Liu, Z.N. Chen, X. Qing, Metamaterial-based low-profile broadband mushroom antenna, IEEE Trans. Antennas Propag. 62 (2014) 1165–1172.
[15] L. Zhu, Exploring strategies for high dielectric constant and low loss polymer dielectrics, J. Phys. Chem. Lett. 5 (2014) 3677–3687.
[16] Z.-M. Dang, Y.-H. Lin, C.-W Nan, Novel ferroelectric polymer composites with high dielectric constants, Adv. Mater. 15 (2003) 1625–1629.
[17] A.D. Yaghjian, Overcoming the Chu lower bound on antenna Q with highly dispersive lossy material, in: 2017 11th European Conference on Antennas and Propagation (EUCAP), IEEE, 2017, pp. 1545–1549.
[18] M. Bakry, L Klinkenbusch, Application of Kramers-Kronig transformations to increase the bandwidth of small antennas, Adv. Radio Sci. 17 (2019) 65–70.
[19] X. Chen, X. Han, Q.-D Shen, PVDF-Based ferroelectric polymers in modern flexible electronics, Adv. Electron. Mater. 3 (2017) 1600460.
[20] P. Petong, R. Pottel, U Kaatze, Dielectric relaxation of H-bonded liquids. Mixtures of ethanol and n-hexanol at different compositions and temperatures, J. Phys. Chem. A 103 (1999) 6114–6121.
[21] D.N. Rander, Y.S. Joshi, K.S. Kanse, A.C Kumbharkhane, Dielectric relaxation and hydrogen bonding interaction in xylitol–water mixtures using time domain reflectometry, Indian J. Phys. 90 (2016) 67–72.
[22] C. Gabriel, S. Gabriel, E.H. Grant, B.S.J. Halstead, P Michael, D. Mingos, Dielectric parameters relevant to microwave dielectric heating, Chem. Soc. Rev. 27 (1998) 213–223.
[23] X. Yang, Y. Huang, L. Chen, A wideband and miniaturized metal rim antenna with a new material for smartphone applications, in: 2022 16th Eur. Conf. Antennas Propagation, EuCAP 2022, 2022, pp. 11–12.
[24] G.G. Raju, Dielectrics in electric fields, Second Edition. Chemical & Engineering News Archive vol. 34, CRC Press, 2016.
[25] K.C. Kao, Electric polarization and relaxation, in: Dielectric Phenomena in Solids, Elsevier, 2004, pp. 41–114.
[26] K. Gohel, D.K. Kanchan, H.K. Machhi, S.S. Soni, C. Maheshwaran, Gel polymer electrolyte based on PVDF-HFP:PMMA incorporated with propylene carbonate (PC) and diethyl carbonate (DEC) plasticizers : electrical, morphology, structural and electrochemical properties, Mater. Res. Express 7 (2020) 025301.
[27] S. Jana, S. Garain, S. Sen, D Mandal, The influence of hydrogen bonding on the dielectric constant and the piezoelectric energy harvesting performance of hydrated metal salt mediated PVDF films, Phys. Chem. Chem. Phys. 17 (2015) 17429–17436.
[28] R. Sarkar, T.K. Kundu, Hydrogen bond interactions of hydrated aluminum nitrate with PVDF, PVDF-TrFE, and PVDF-HFP: A density functional theory-based illustration, Int. J. Quantum Chem. 120 (2020) 1–23.
[29] T.V. Terziyan, A.P. Safronov, Solubility and H-bonding of poly(vinylidene fluoride) copolymers in carbonyl liquids: Experiment and molecular simulation, J. Mol. Liq. 275 (2019) 378–383.
[30] S. Kim, et al., High discharge energy density and efficiency in newly designed PVDF@SiO 2 –PVDF composites for energy capacitors, ACS Appl. Energy Mater. 3 (2020) 8937–8945.
[31] P. Martins, A.C. Lopes, S. Lanceros-Mendez, Electroactive phases of poly(vinylidene fluoride): Determination, processing and applications, Prog. Polym. Sci. 39 (2014) 683–706.
[32] J. Li, Q. Meng, W. Li, Z. Zhang, Influence of crystalline properties on the dielectric and energy storage properties of poly(vinylidene fluoride), J. Appl. Polym. Sci. 122 (2011) 1659–1668.
[33] Y. Huang, K. Boyle, Antennas 363 (2008).
[34] A. Nakayama, H. Yoshikawa, Observation of dielectric dispersion of BaTiO3 ceramics in the gigahertz frequency region by scattering parameter measurement using a pair of surface electrodes, Appl. Phys. Lett. 95 (2009) 072904.
[35] M. Lente, J.d.L.S. Guerra, J. Eiras, S. Lanfredi, Investigation of microwave dielectric relaxation process in the antiferroelectric phase of NaNbO3 ceramics, Solid State Commun. 131 (2004) 279–282.
[36] V. Porokhonskyy, D. Damjanovic, Domain wall contributions in Pb(Zr,Ti)O3 ceramics at morphotropic phase boundary: a study of dielectric dispersion, Appl. Phys. Lett. 96 (2010) 242902.
[37] M. Qin, L. Zhang, H Wu, Dielectric loss mechanism in electromagnetic wave absorbing materials, Adv. Sci. 9 (2022) 2105553.
[38] Y. Li, et al., Vertical interphase enabled tunable microwave dielectric response in carbon nanocomposites, Carbon 153 (2019) 447–457.
[39] L.-M. Wang, R Richert, Identification of dielectric and structural relaxations in glass–forming secondary amides, J. Chem. Phys. 123 (2005) 054516.
[40] Z. Wang, et al., Data-driven materials innovation and applications, Adv. Mater. 2104113 (2022).
[41] R. Batra, L. Song, R. Ramprasad, Emerging materials intelligence ecosystems propelled by machine learning, Nat. Rev. Mater. 6 (2021) 655–678.
[42] L. Chen, et al., Frequency-dependent dielectric constant prediction of polymers using machine learning, npj Comput. Mater. 6 (2020) 30–32.
[43] J. Qin, Z. Liu, M. Ma, Y. Li, Machine learning approaches for permittivity prediction and rational design of microwave dielectric ceramics, J. Materiom. 7 (2021) 1284–1293.
[44] M. Zhu, T. Deng, L. Dong, J. Chen, Z. Dang, Review of machine learning-driven design of polymer-based dielectrics, IET Nanodielectr. 5 (2022) 24–38.
[45] CST Studio Suite 3D EM simulation and analysis software. http://www.cst.com.